CORROSION SCIENCE AND TECHNOLOGY, Vol.23, No.2(2024), pp.121~130 pISSN 1598-6462 / eISSN 2288-6524
[Research Paper] DOI: https://doi.org/10.14773/cst.2024.23.2.121

New Corrosion-Resistant Zn-Al-Mg Alloy Hot-Dip Galvanized Steel Sheet

Kohei Tokuda[1,†], Yasuto Goto[1], Mamoru Saito[2], Hiroshi Takebayashi[2], Takeshi Konishi[2], Yuto Fukuda[3], Fumiaki Nakamura[4], Koji Kawanishi[4], Kohei Ueda[2], and Hidetoshi Shindo[3]

[1]*Nippon Steel Corporation Technical Research & Development Bureau Setouchi R&D Lab., Himeji/ Hyogo, 671-1188, Japan*
[2]*Nippon Steel Corporation Technical Research & Development Bureau R&D Lab., Futtsu/ Chiba, 293-8511, Japan*
[3]*Nippon Steel Corporation Setouchi Works.,Himeji/ Hyogo, 671-1188, Japan*
[4]*Nippon Steel Corporation Flat Products Marketing Div.,Chiyoda-Ku/Tokyo, 100-0005, Japan*
(Received January 25, 2024; Revised March 26, 2024; Accepted March 27, 2024)

In recent years, Zn-Al-Mg alloy galvanized steel sheets have been widely used as coated steel sheets to support social capital in the infrastructure field. A feature of Zn-Al-Mg alloy-coated steel sheets is that they provide a better corrosion protection period than Zn-coated steel sheets. In this study, the corrosion resistance of a new Zn-Al-Mg alloy-coated steel sheet was investigated and compared to that of conventional commercially available coated steel sheets. The investigation confirmed that increasing the Mg concentration in the Zn-Al-Mg-coated steel sheet improved corrosion resistance, which was more than 10 times that of the galvanized steel sheet specified in JIS G 3302. The study findings also confirmed that the corrosion resistance reached more than twice that of the coated steel sheet specified in JIS G 3323. If such galvanized steel sheets are applied to social infrastructures that are exposed to severely corrosive environments, the service life of the infrastructure might be extended.

Keywords: *Hot-dip galvanized steel sheets, Zn-Al-Mg, Corrosion mass loss, Mg effects*

1. Introduction

Hot-dip galvanizing is widely used as an economical method of preventing corrosion of steel materials in the construction and civil engineering market. It is said that continuous hot-dip galvanized steel sheets were first produced in Japan in 1883. In recent years, the concept of life cycle cost, which includes not only the initial cost of parts but also the maintenance cost during the period of usage, has become widespread. As a result, there is a strong demand in the market for hot-dip zinc-coated steel sheets with high corrosion resistance that can reduce maintenance labour and costs. Under these circumstances, around the year 2000, Zn-Al-Mg coated steel sheets containing a small amount of Mg were developed. Currently, Zn-6mass%Al-3mass%Mg alloy coated steel sheets (ZAM™) and Zn-11mass%Al-3mass%Mg-0.2mass%Si alloy coated steel sheets (SuperDyma™) are manufactured in Japan. Zn-Al-Mg alloy coated steel sheets (JIS G 3323) in which alloying elements such as Al and Mg are added to the Zn coating layer are commonly used for the purpose of long-term durability of steel materials. Therefore, focusing on the chemical composition of the Zn-Al-Mg coated steel sheets that have been studied for production Most of the cases were Al concentration up to 11% and Mg concentration up to 3%, and Zn-Al-Mg coated steel sheets exceeding this composition range have hardly been studied. At this time, as a result of examining coating compositions that exceed the conventional composition examination range, Zn-19mass%Al-6mass%Mg-Si coated steel sheets (ZEXEED™) [4] that has more than doubled the corrosion resistance of the conventional hot-dip Zn-Al-Mg coated steel sheets was found. Commercial production of this coated steel sheet began in October 2021. In other words, it means that the technological evolution of highly corrosion-resistant hot-dip galvanized steel sheets has moved to the next step. In this report, we discuss the performance change of the coating layer caused by the addition of Al and Mg. In addition, the excellent corrosion resistance and corrosion process of the ZEXEED™ are compared with the conventional Zn-Al-Mg coated steel sheet SuperDyma™.

†Corresponding author: tokuda.m8e.kohhei@jp.nipponsteel.com

2. Experimental Method

2.1 Materials

A total of 26 coating compositions were tested for corrosion resistance evaluation, and Table 1 shows the alloy components of 21 major composition points. These alloys were melted in the melting furnace of our company's complete nitrogen-replacement type hot-dip galvanized simulator, whose schematic diagram is shown in Fig.1, and were kept at the respective set bath temperatures in Table1. A cold-rolled steel sheet (JIS G 3141) of 200 × 100 × 0.8 mm or a hot-rolled steel sheet (JIS G 3131) of 200 × 100 × 3.2 mm was used as the base sheet for galvanizing. The steel substrate was thoroughly degreased and pickled, washed with distilled water, and dried before hot-dipping. The steel sheets were placed in a sample holder in the hot-dip simulator. The sample box was completely purged with nitrogen before the hot-dipping, and the oxygen concentration around melting pot and chamber in the hot-dip simulator was kept below 20 ppm until the end of hot-dipping process. A K thermocouple was spot-welded to the centre of the back surface of the steel sheet to enable monitoring and control of the temperature in a series of processes from the start to finish of manufacturing the coated steel sheet. Both 0.8 mm and 3.2 mm steel sheets were annealed and reduced at 1073K in a N_2-4 vol%H_2 reducing atmosphere for 1 min. After that, the steel sheet was cooled down to the coating bath temperature with N_2 gas. Then, it was immersed in the coating bath and stay for 3 seconds. Here, while pulling up, the N_2 gas wiping flow rate and pressure were adjusted to control the coating thickness to about 20 to 30 μm. Finally, as a cooling process, N_2 gas was blown so that the average cooling rate from the melting point to 100 K was 10 to 15 K/sec.

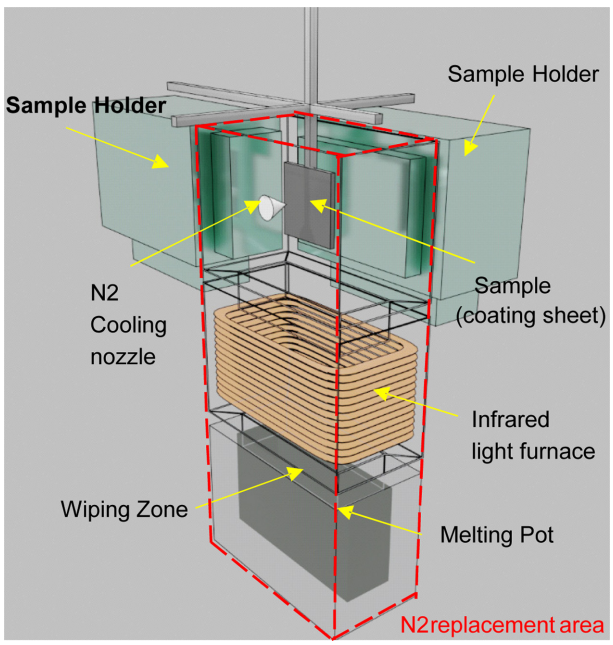

Fig. 1. Hot-dip coating simulator

Table 1. Chemical composition and temperature of Zn-Al-Mg baths

No.	Bath symbols	Composition (mass%)				Bath Temperature (K)	No.	Bath symbols	Composition (mass%)				Bath Temperature (K)
		Zn	Al	Mg	Si				Zn	Al	Mg	Si	
1	19Al16Mg	bal.	19.0	6.0	0.2	773	12	I	bal.	19.0	6.5	0.2	500
2	11Al13Mg	bal.	11.0	3.0	0.2	723	13	J	bal.	19.0	7.0	0.2	500
3	Zn-0.2Al	bal.	0.2	0.0	0.0	723	14	K	bal.	19.0	7.5	0.2	500
4	A	bal.	2.0	2.0	0.0	723	15	L	bal.	19.3	8.5	0.2	500
5	B	bal.	5.0	1.0	0.0	723	16	M	bal.	25.0	6.0	0.2	530
6	C	bal.	6.0	3.0	0.0	723	17	N	bal.	27.1	11.0	0.2	550
7	D	bal.	6.5	11.0	0.0	723	18	O	bal.	30.0	6.0	0.2	550
8	E	bal.	9.0	5.8	0.0	723	19	P	bal.	30.0	8.0	0.2	550
9	F	bal.	11.3	4.7	0.0	723	20	Q	bal.	35.0	8.0	0.2	550
10	G	bal.	13.8	5.8	0.0	723	21	R	bal.	35.0	2.0	1.6	600
11	H	bal.	14.4	14.0	0.0	773							

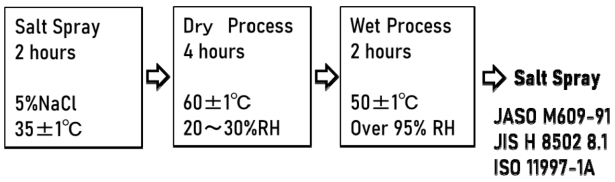

Fig. 2. CCT mode in this test

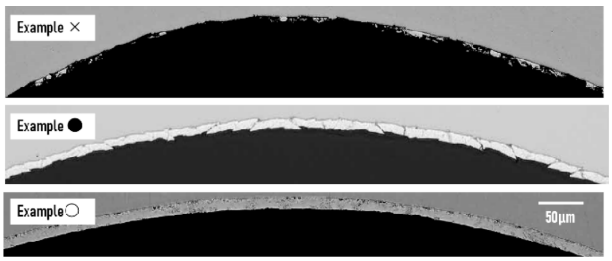

Fig. 3. Example of powdering peeling on the inner surface of 5R-90°bent samples

2.2 Corrosion test

Several 100 × 50 × 0.8 mm pieces were cut from the centre of the coated steel sheet, and the edge of the sample was stamped, and the weight of the sample before the corrosion test was measured. The perimeter of the cut edge of the steel sheet was sealed with polyester adhesive tape (No. 31 B manufactured by Nitto Denko Co.), and then corrosion evaluation surface area (70 × 40 mm) was formed. The specimens were put into the cyclic corrosion tester, operated in JASO mode (Neutral salt spray cycle test method specified in 8.1 of JIS H 8502 Japan Automotive Technical Standard M609-91(Fig. 2), and corrosion tests were continued up to 900 cycles. All samples were subjected to corrosion mass loss measurements at JASO 60 cycles. Corrosion mass loss evaluation proceeds as follows. The tape seal of the test sample after corrosion test was peeled off and immersed in a 30% chromic acid (VI) aqueous solution at 296K for 10 minutes. Remove the corrosion products formed on the coated surface by lightly rubbing the corrosion evaluation surface with a sponge while rinsing with water. After thoroughly washing and drying, the weight was measured with an electronic balance to measure the corrosion mass loss per unit area (g/m^2) after the corrosion test. Weight measurements were performed for 19Al6Mg and 11Al3Mg after 9, 15, 27, 30, 45, 60, 90, 120 and 180 cycles. Corrosion tests were continued for 19Al6Mg up to 900 cycles and 11Al3Mg up to 600 cycles. Weight measurement was done for Zn-0.2Al after 9, 15, 27, 30, 45, 60 cycles, and the corrosion test was stopped after 90 cycles due to the red rust of the surface.

2.3 Exposure Test for Cutting Edge of Coating Steel Sheets

The 3.2 mm coated steel plates of 19Al6Mg and 11Al3Mg were cut into 100 × 50 mm pieces by shearing. A φ11 mm bolt fixing hole was drilled under the steel plate. It was fixed on an exposure stand at an angle of 60 degrees from the horizontal at the exposure field in Futtsu City, Chiba Prefecture, Japan, Photographs of the side surface of the steel plate were taken periodically, and the red rust area ratio on the side surface of the steel plate (ratio of red rust area to a cut edge area of 100 × 3.2 mm) was calculated by computer analysis from the images.

2.4 Hardness and formability of Coating Steel Sheets

Hardness was measured from the coating layer surface using a micro Vickers hardness tester (Mitsutoyo-HM 221). A total of 30 measurements were taken on the surface of the coating layer in an area of 25 × 8 mm at equal intervals of 5 mm long and 2 mm wide, and the average value was taken as the Vickers hardness. The test load was 10gf. Furthermore, the steel sheets were cut into 50 × 90 × 0.8 mm, and press-formed at 5R-90° so that the bent parts were the centre of the base sheets width and perpendicular to the longitudinal direction of the sheets. The bent portion was embedded in resin as it was, and the cross section of the inner surface of the bent central portion was observed to confirm the presence or absence of cracks and peeling of the coating layer (Fig. 3), and the coating formability was evaluated as follows.

(1) coating layer without cracks and peeling (judgment ○)
(2) Cracks are observed, but there is no peeling of the coating layer (judgment ●)
(3) Peeling is seen inside the coating layer (judgment ×)

2.5 XRD Analysis

For 19Al6Mg and 11Al3Mg, samples of 25 × 25 × 0.8 mm were cut from the central part of the corroded test pieces after the predetermined JASO cycles had

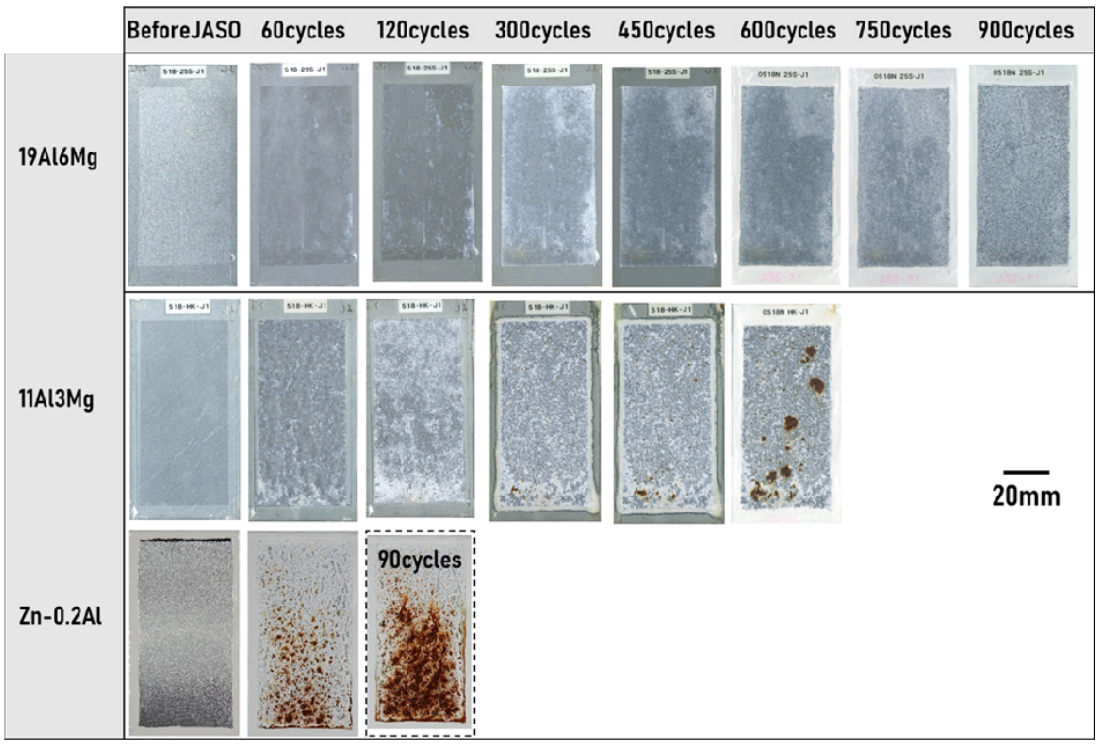

Fig. 4. Sample external appearances after CCT

passed. XRD was used to identify the remaining coating layer and the formed corrosion products. RINT1500 manufactured by RIGAKU was used for XRD measurement. The target was Cu, the acceleration voltage was 40 kV, 300 mA, the diffraction angle measurement range was 5 to 90 degrees (2θ), and the measurement interval was 0.05 degrees.

2.6 Hot-dip Zinc Exposure Test

Hot-dip Zn-coated steel sheets of 150 × 70 × 4.5 mm (Zn coating weight of 450 g/m^2 or more, HDZT63, JIS H 8641 standard product, which means the most common batched 100% Zinc hot-dip coatings) were prepared to confirm the corrosion products formed on the Zn coating in the exposure test. It was exposed to sunlight outside for 3 years at an angle of 30 degrees from the horizontal, facing south, in Okinawa Prefecture, Japan. After the exposure test, a 20 mm square sample was cut from the canter of the surface of the plated steel sheet, and the corrosion products formed on the surface of the coating layer were analysed by the XRD method described in Section 2.5 to identify the formed corrosion products.

3. Results

3.1 Corrosion test

Fig. 4 shows the corrosion appearance of 19Al6Mg, 11Al3Mg, and Zn-0.2Al after the JASO corrosion test. In 19Al6Mg, no red rust occurred up to 900 cycles. In 11Al3Mg, red rust formation was confirmed below the evaluation surface at 450 cycles, and the red rust area widened at 600 cycles. In Zn-0.2Al, red rust was observed at the 60th cycle, and red rust occurred almost all over the surface at the 90th cycle. Fig. 5 shows the changes in corrosion mass loss for 19Al6Mg, 11Al3Mg and Zn-0.2Al. The corrosion mass loss of 19Al6Mg remained at half that of 11Al3Mg up to JASO 180 cycles. Fig. 6 shows the corrosion mass loss of various coating layers in the JASO 60 cycle. Multiple regression analysis was performed using the obtained corrosion mass loss values. If the corrosion mass loss in JASO 60 cycles is a function of Al concentration and Mg concentration (mass%), the results can be expressed by the following equation.

$$CML=74.24 - 1.20[Al] - 5.26[Mg] \quad (1)$$

However, multiple correlation R = 0.77 in (equation (1)), (WML: g/m^2) is the corrosion mass loss of the coating layer in the JASO 60 cycle, [Al] is the Al component composition (mass%) in the coating layer, and [Mg] is the Mg component composition (mass%) in the coating layer. Fig. 7 shows the transition of the red rust area ratio on the cut edge of 3.2 mm. 19Al6Mg had a lower red rust area ratio than 11Al3Mg throughout the period. On the 100th day, the red rust area ratio reached a maximum and became equivalent to that of 11Al3Mg, but the red rust area ratio immediately decreased after that. After 200 days, the red rust area ratio was almost 0%. For 11Al3Mg, the red rust area ratio fluctuated up to 60 days of exposure test, and reached a maximum around 30 days. After that, the red rust area ratio decreased temporarily after 100 days, but increased again after 180 days. Around 365 days, the red rust area ratio was less than 10%, and after that, the red rust area ratio was almost 0% until 730 days.

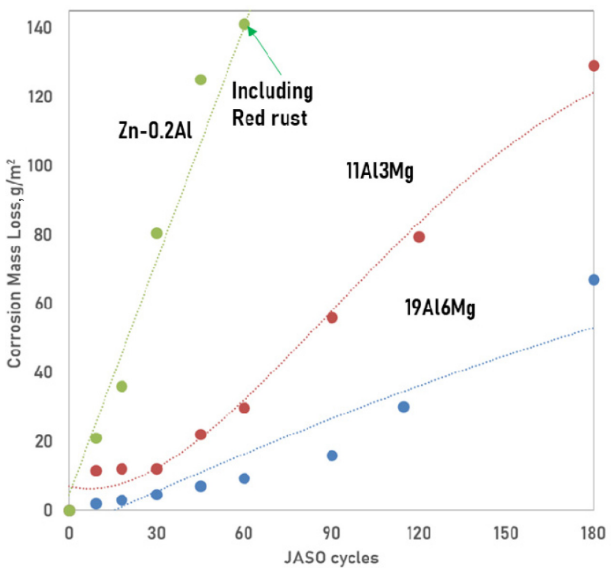

Fig. 5. Corrosion mass losses of Zn-Al-Mg coatings

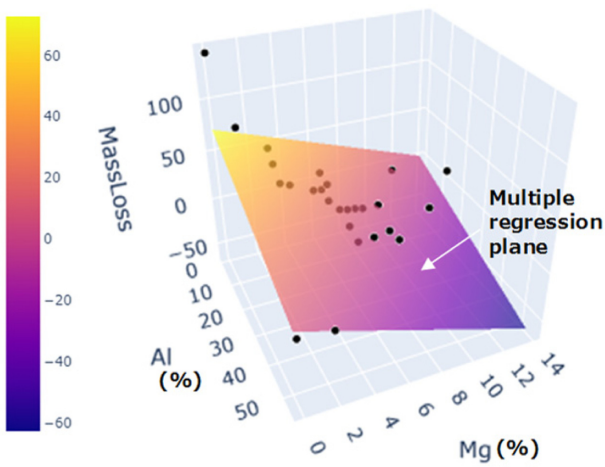

Fig. 6. Corrosion mass loss of Zn-Al-Mg coatings

3.2 Hardness and formability

Fig. 8 shows the relationship between Mg concentration and Vickers hardness. It was confirmed that the Vickers hardness increased as the Mg concentration in the coating layer increased, and the relationship between Mg% and Vickers hardness could be approximated by a quadratic function. When the Mg concentration was less than 4%, no cracks or peeling of the coating layer were observed on the inner surface of the coating layer with 5R-90° bending. Cracks were observed on the inner surface of the coating layer up to 7.5%, but no peeling

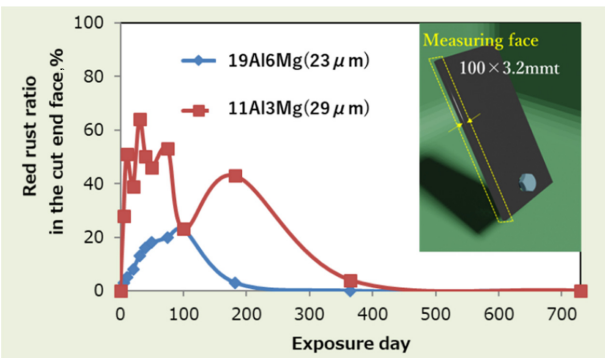

Fig. 7. The transitions of red rust ratio in cutting end face of 3.2 mm 19Al6Mg and 11Al3Mg in Futtsu, Japan

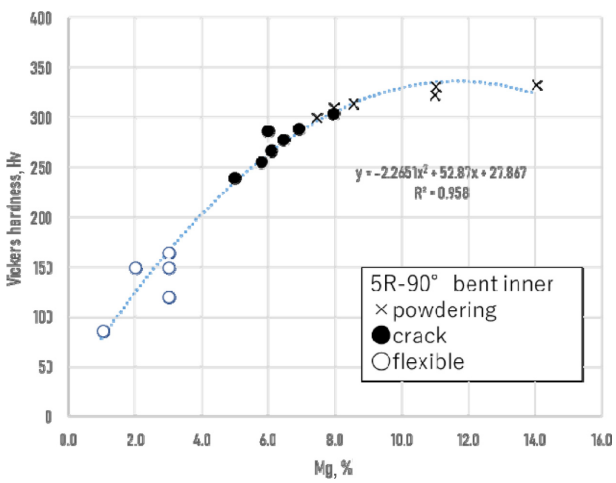

Fig. 8. Relationship between Mg % and Vickers hardness

occurred. However, when the Mg concentration was 7.5% or more, peelings of the coating layer were confirmed, and peelings began to occur when the Vickers hardness reached 300 Hv. From the above, it is considered that there is a composition point between 7% and 7.5% at which the coating layer begins to peel off.

3.3 Corrosion products

3.3.1 Corrosion products on the 19Al6Mg and 11Al3Mg in JASO test

Fig. 9 shows the XRD diffraction pattern after JASO. $Zn_5(OH)_8Cl_2 \cdot H_2O$(Simonkolleite) and ZnO(Zincite) were detected at 120 cycles, and $Zn_2Al(OH)_6Cl \cdot 1.8H_2O$ was additionally detected at 300 cycles. At 450 cycles, the amount of Simonkolleite detected decreased, and $Zn_6Al_2(OH)_{16}CO_3 \cdot 4H_2O$ was detected instead. In addition, the peak intensity of Zincite also increased. $Mg_6Al_2(CO_3)(OH)_{16} \cdot 4H_2O$(Hydrotalcite) was confirmed. However, the peak intensity was small. Hydrotalcite could not be detected after 600 cycles. Changes in the XRD diffraction pattern between 600 and 750 cycles were small, but $Zn_5(OH)_6(CO_3)_2$(Hydrozincite) was detected as a new corrosion product at 900 cycles. Diffraction peaks due

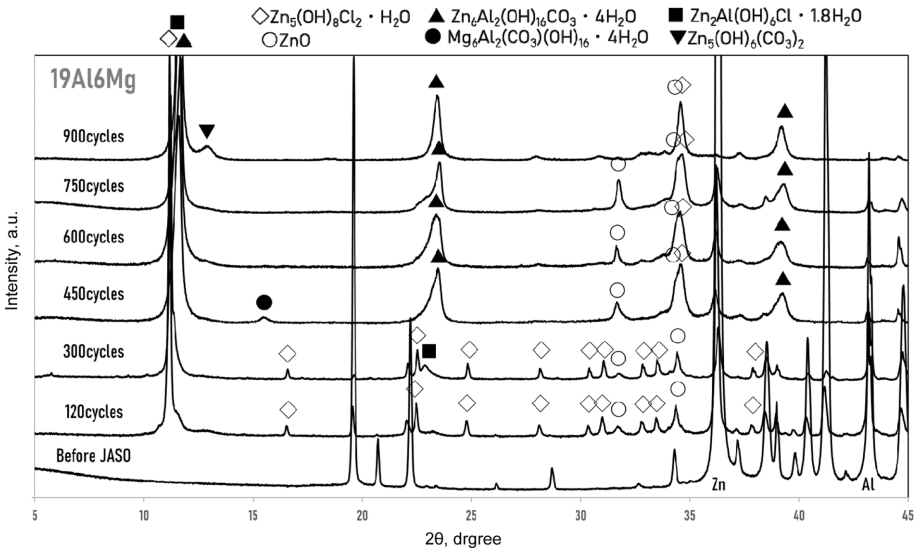

Fig. 9. XRD patterns of 19Al6Mg after JASO

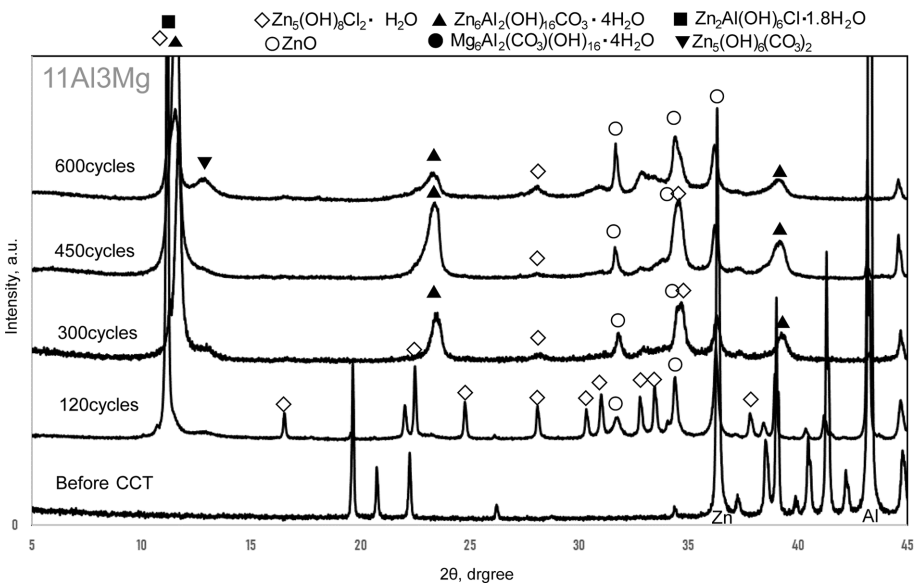

Fig. 10. XRD patterns of 11Al3Mg after JASO

to Zn (near 2θ= 36°) and Al (near 2θ = 43°) were not detected at 900 cycles unlike the samples after other cycles. Fig. 10 shows the XRD diffraction pattern of 11Al3Mg after JASO. Corrosion products of 11Al3Mg detected throughout the cycle are similar to those of 19Al6Mg. At 120 cycles, the formation of Simonkolleite and Zincite was confirmed as well as 19Al6Mg. At 300 cycles, the diffraction peak intensity of Simonkolleite decreased faster than that of 19Al6Mg. $Zn_6Al_2(OH)_{16}CO_3{\cdot}4H_2O$ was detected instead. The change in the X-ray diffraction pattern was small from 300 cycles to 450 cycles, and Hydrozincite was detected at 600 cycles, and diffraction peaks due to Zn and Al were not detected.

3.3.2 Corrosion products on the HDZT63 in 3-year exposure test

Fig. 11 shows the XRD diffraction pattern of HDZT63 exposed to the Okinawa region for 3 years. $Zn_5(OH)_8Cl_2$, ZnO, $Zn_5(OH)_6(CO_3)_2$, etc. were detected as main corrosion products on the surface of the Zn hot-dip coating layer.

4. Discussion

4.1 Corrosion resistance of Zn-Al-Mg coatings

From the change curve of corrosion weight loss shown in Fig. 5, it can be seen that the corrosion rate of Zn-Al-Mg alloy coating is lower than that of Zn-0.2Al, and that of 19Al6Mg is lower than that of 11Al3Mg. The Zn-0.2Al coating layer, which consists of a single Zn phase, has a very high corrosion rate. In addition, from the corrosion appearance shown in Fig. 4, considering that the amount of corrosion products formed on the coating layer surface at 120 cycles is small, the main reason for the improvement in corrosion resistance of Zn-Al-Mg alloy coating is considered to be the change in the constituent phases from the Zn phase due to the addition of Al and Mg. CML=74.24-1.20[Al]-5.26[Mg] (equation (1)), which was derived from Fig. 6 by multiple regression analysis, shows that Mg is more effective than Al in reducing corrosion mass loss. An increase in the Al content in the coating layer causes an increase in the Al-Zn phase (a mixed phase of fine Al and Zn phases) in the coating layer [5]. An increase in Mg forms a ternary eutectic structure (mixed phase) with Zn, Al, and $MgZn_2$ phases, and the Mg concentration away from the eutectic composition causes coarsening of the $MgZn_2$ phase [6]. On the other hand, it causes a decrease in the Zn phase contained in the ternary eutectic structure. In other words, the corrosion resistance is improved by changing the Zn phase in the ternary eutectic structure into Al–Zn phase or $MgZn_2$ phase. Therefore, Mg, which directly binds to Zn and reduces the phase content, is more effective than Al, which forms a mixed phase with Zn.

4.2 Optimum composition

From the viewpoint of corrosion resistance, increasing Al and Mg concentrations is preferable. However, in

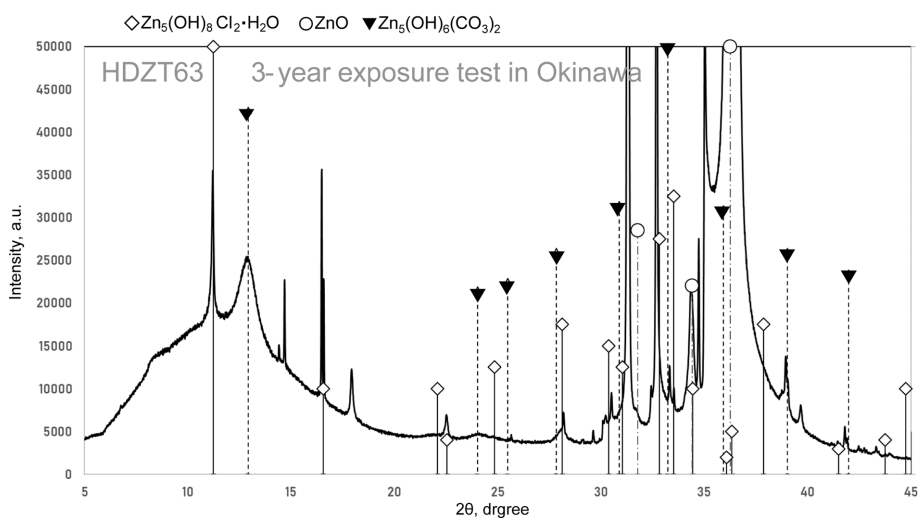

Fig. 11. XRD pattern of HDZT63 after 3-year exposure test in Okinawa

general, when the Al content increases, excellent corrosion resistance is obtained with a small corrosion rate of the Al phase caused by the Al_2O_3 film in all coating layers, but the sacrificial corrosion resistance decreases at cut edges and scratches. Fig. 7. compares the sacrificial corrosion resistance of the coating layer on the cut edge. 19Al6Mg is superior to 11Al3Mg in sacrificial corrosion resistance. This means that the decrease in sacrificial corrosion resistance due to the increase in Al concentration was offset by the Mg added at the same time, and it can be seen that the sacrificial corrosion resistance is improved. On the other hand, Fig. 8. shows that the coating hardness increases, and formability tends to deteriorate with increasing Mg concentration. Therefore, when aiming at a coated steel sheet with high versatility, the concentration of Mg addition should be limited. Considering the balance between corrosion resistance, sacrificial corrosion resistance, and formability, Zn-19%Al-6%Mg is selected as the optimum composition.

4.3 Corrosion mechanism determined from corrosion products

From Fig. 4, it can be confirmed that 19Al6Mg has a very long red rust inhibition period. As can be seen from Fig. 9, Zn and Al are detected in 19Al6Mg up to 750 cycles, and the metallic phase of the coating layer remains under the corrosion products. On the other hand, in 11Al3Mg, Zn and Al phases were detected until around 450 cycles, after which red rust started to become conspicuous at 600 cycles. When corrosion reaches the base steel, the coating layer sacrificially prevents corrosion of the base steel. In other words, in order to suppress red rust, it is necessary to leave metallic phases such as Al and Zn in the coating layer for a long period of time, and 19Al6Mg is superior to 11Al3Mg in the sustainability of this effect. Here, focusing on the types of corrosion products, the corrosion products formed by JASO in 19Al6Mg and 11Al3Mg are the same except for $Mg_6Al_2(CO_3)(OH)_{16}\cdot 4H_2O$ (Hydrotalcite). This is illustrated in Fig. 12 First, regarding the transition of corrosion products of Zn-based coating, a past study [7] indicates that Simonkolleite changes to Zincite through Hydrozincite. Corrosion products similar to those found in the past were also confirmed in the Okinawa exposure test (Fig. 11) using hot-dip Zn coating plate, which means that similar corrosion products tend to form in the exposure test and JASO. Based on this fact, the transitions of the corrosion products formed in the exposure test of the Zn-Al-Mg coatings is discussed. Among these three types of corrosion products, Simonkolleite and Zincite are detected as corrosion products in existing literature [8], and it is also shown that $Zn_6Al_2(OH)_{16}CO_3\cdot 4H_2O$ is also formed. Therefore, comparing Fig. 9 and Fig. 10 with the exposure test, it can be confirmed that the transitions of the corrosion products in Zn-Al-Mg coatings formed by JASO are also similar. Due to the high corrosion resistance of Zn-

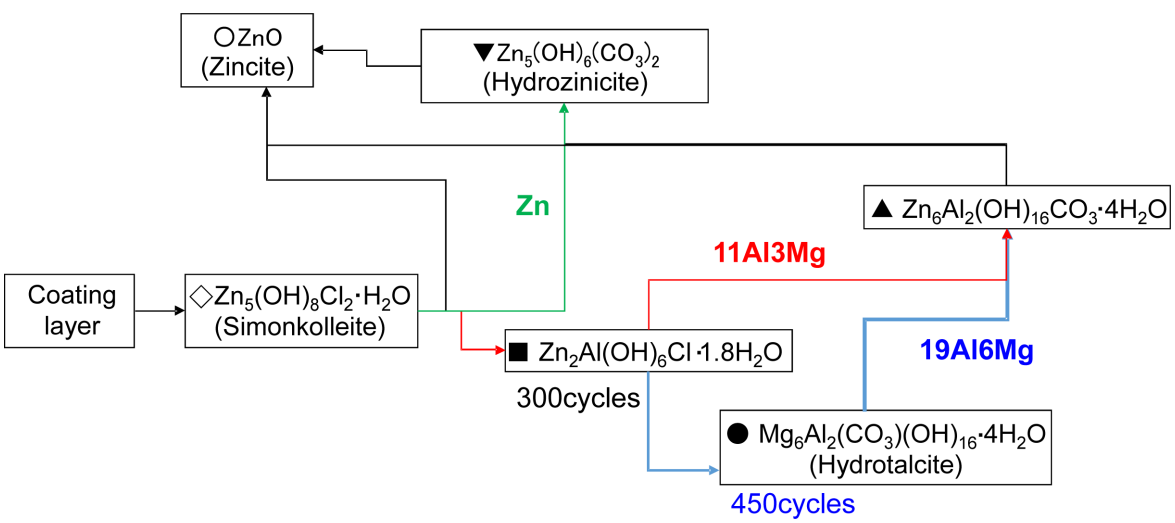

Fig. 12. Transition of corrosion products in JASO

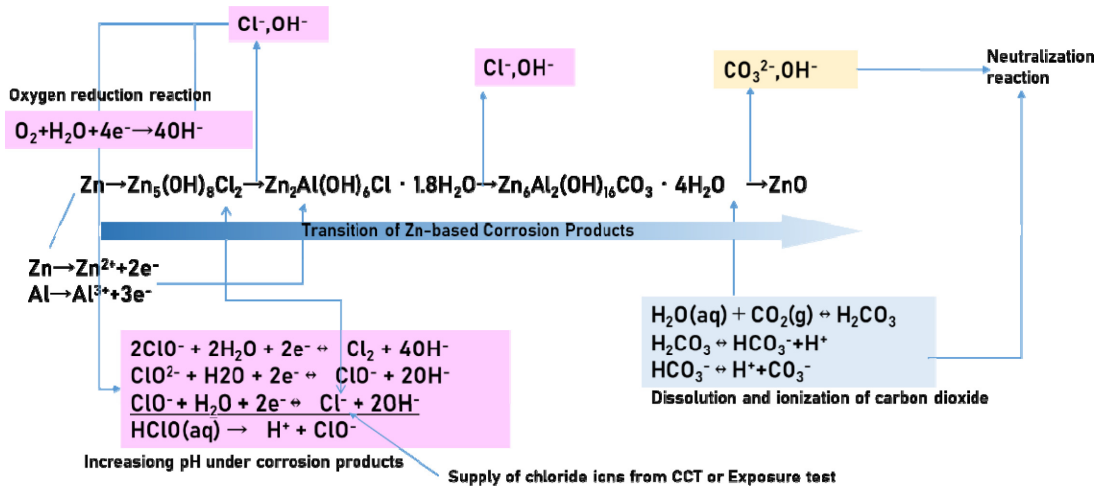

Fig. 13. Ionic reaction formulas related to the transition of Zn-based corrosion products

Al-Mg coatings, it is difficult to estimate the corrosion mechanism up to the life ending of the coating layer in exposure tests. Therefore the corrosion mechanism of JASO, which is an accelerated corrosion test, is close to the exposure test, it has been shown to be an effective means for examining the exact corrosion mechanism of the coating layer. Focusing on the transition of corrosion products, 19Al6Mg shows a more complex transition from Simonkolleite to ZnO than 11Al3Mg. The amount of Al^{3+} and Mg^{2+} ions supplied increases during the corrosion process, and as a result, corrosion products such as $Mg_6Al_2(CO_3)(OH)_{16}\cdot 4H_2O$ (Hydrotalcite), which are not confirmed for 11Al3Mg, are also formed. Here, Fig. 13 shows the possible ion reaction and electrolytic dissociation equilibrium examples involved in the transformation Zn-based corrosion products from Simonkolleite to ZnO. This transition is promoted by carbon dioxide present in the atmosphere, and at the same time, the OH^- ions contained in the corrosion products are separated and the corrosion products are neutralized. In Zn-Al-Mg coatings, on the other hand, corrosion products containing Al and Mg are formed during the corrosion process, which is thought to inhibit the progress of the neutralization reaction. This means that the high pH condition is maintained for a long time under the corrosion products. As a result, the dissolution rate of Mg may decrease due to the passivation of Mg, and the Fe anode reaction of the base steel may be suppressed. Therefore, it is considered that the role of Al and Mg contributes to the suppression of excessive corrosion promotion of the coating layer due to sacrificial corrosion resistance, and changes the Zn coating to a structure that can protect the base steel for a long period of time. However, further detail research is necessary to clarify the correct transition process

5. Conclusion

The optimum composition of Zn-Al-Mg coating was investigated by JASO test, exposure test and processing test. In addition, the corrosion mechanism was discussed from the transition of corrosion products formed on each coating layer.

(1) In Zn-Al-Mg coating, the results of JASO show that the corrosion resistance is improved by increasing the Al and Mg concentrations. Mg has a greater effect of improving corrosion resistance than Al.

(2) The sacrificial corrosion resistance of 19Al6Mg is superior to that of 11Al3Mg, and the increase in Mg concentration offsets the decrease in sacrificial corrosion resistance due to the increase in Al concentration.

(3) An excessive increase in Mg concentration impairs the formability of the coated steel sheet.

(4) Considering the balance between corrosion resistance, sacrificial corrosion resistance and formability, 19Al6Mg is considered to be the optimum composition.

(5) Corrosion products were confirmed by JASO, and

it was confirmed that the corrosion products formed on 19Al6Mg were similar to those of Zn-based coating and 11Al3Mg.

(6) The transition of corrosion products of 19Al6Mg is more complicated than that of Zn-based coating and 11Al3Mg.

(7) 19Al6Mg retains corrosion products for a long time. As a result, it is thought that the pH under the corrosion products is kept high, and the corrosion of the coating layer and the base steel is suppressed.

References

1. Y. Hisamatsu, History of Hot-Dip Galvanized Sheet in Japan, *The Journal of the Metal Finishing Society of Japan*, **34**, 354 (1983). Doi: https://doi.org/10.4139/sfj1950.34.354
2. A. Komatsu, H. Izutani, T. Tsujimura, A. Andoh, T. Kitaka, Corrosion Resistance and Protection Mechanism of Hot-dip Zn-Al-Mg-Alloy Coated Steel Sheet under Accelerated Corrosion Environment, *Tetsu-to-Hagané*, **86,** 534 (2000). Doi: https://doi.org/10.2355/tetsutohagane1955.86.8_534
3. Y. Morimoto, M. Kurosaki, K. Honda, K. Nishimura, S. Tanaka, A. Takahashi, H. Shindo, The Corrosion Resistance of Zn-11% Al-3% Mg-0.2% Si Hot-dip Galvanized Steel Sheet, *Tetsu-to-Hagané*, **89**, 161 (2003). Doi: https://doi.org/10.2355/tetsutohagane1955.89.1_161
4. K. Tokuda, M. Saito, Y. Goto, F. Nakamura, Y. Ishida, K. Matsumura, New Corrosion Resistant Coated Steel "ZEXEED™", *NIPPON STEEL TECHNICAL REPORT,* **129**, 63 (2023). https://www.nipponsteel.com/common/secure/en/tech/report/pdf/129-13.pdf
5. T. Mitsunobu, K.Tokuda, N.Shimoda, Peritectic Structure Evolution in Hot-dip Zn-Al Alloy Coatings, *Tetsu-to-Hagané,* **106**, 254 (2020). Doi: https://doi.org/10.2355/tetsutohagane.TETSU-2019-107
6. W. Yamada, K. Honda, K. Tanaka, H. Hatanaka, K. Ushioda, Solidification Structure of Coating Layer in Hot-dip Zn-11% Al-3% Mg-0.2% Si-coated Steel Sheet and Phase Diagram of the System, *NIPPON STEEL TECHNICAL REPORT,* **102**, 37 (2013). https://www.nippon-steel.com/en/tech/report/nsc/pdf/102_08_Yamada.pdf
7. H. Hamada, T. Deguchi, Aenkei Fushoku Seiseibutu no Seisei Kikou, *Rust prevention & control,* **38**, 453 (1994).
8. K. Ueda, A. Takahashi, Y. Kubo, Investigation of corrosion resistance of pre-painted Zn-11% Al-3% Mg-0.2% Si alloy coated steel sheet through outdoor exposure test in Okinawa, *La Metallurgia Italiana*, **104**, 13 (2012). https://www.fracturae.com/index.php/aim/article/view/261/231